Journal of Structural Geology, Vol. 10, No. 7, pp. 717 to 734, 1988
Printed in Great Britain

0191-8141/88 $03.00 + 0.00

Deformational and strain patterns of an intracontinental collision ductile shear zone—an example from the Higher Garhwal Himalaya

A. K. JAIN

Department of Earth Sciences, University of Roorkee, Roorkee—247 667, India

and

ARVIND ANAND

2051, 49 AST, Edmonton, Alberta, Canada T6L 2WG

(*Received* 31 *May* 1987; *accepted in revised form* 15 *June* 1988)

Abstract—The Higher Himalayan metamorphic belt of Garhwal appears to have evolved in a major 15–20 km wide, NE-dipping ductile shear zone of the overthrust-type due to intracontinental crustal shortening during Cenozoic continental collision within the Indian Plate. Out of the four major distinct deformation phases, the most widespread D_2 deformation phase is marked by a prominent S_2 foliation axial-planar to the reclined and recumbent F_2 folds, a coaxial NE-plunging L_2 stretching lineation and syntectonic growth of index metamorphic minerals. These deformational structures are developed during the SW-directed D_2 ductile shear deformation, irrespective of the orientation of the S_2 foliation and thrust zones.

Regional strain patterns in quartzite of the Lesser Himalayan Garhwal Group beneath the Main Central Thrust (MCT) and the Central Crystalline Zone using R_f/ϕ data on quartz clasts and aggregates reveal that the maximum values of finite strain $\bar{\varepsilon}_s$ are attained within narrow mylonitic shear zones within the broad ductile shear zone. During its progressive translation towards higher structural levels in late D_2 and D_3 deformation phases, the shortening was accommodated by development of thrust sheets with the MCT and Jutogh Thrust surfaces coinciding with zones of mylonite and maximum strain. At higher levels, ductile shear zones became compressional brittle–ductile zones which resulted in the development of SW-verging F_{3a} and F_{3b} folds during the southward migration of the thrust sheets in the Lesser Himalaya.

INTRODUCTION

RECENT studies have shown that subduction of the oceanic crust of the Indian Plate beneath the Eurasian Plate during the late Cretaceous to Eocene along the Indus–Tsangpo Suture Zone (ITSZ) was followed by collision of the Indian continent with Eurasia (Brookfield & Reynolds 1981, Honegger *et al.* 1982, Coward *et al.* 1986, Searle 1986, Thakur 1987). The continental collision has considerably deformed the Higher Himalayan basement metamorphic rocks due to intracontinental crustal shortening and southward thrusting along the Main Central Thrust (MCT) and associated thrusts over the Lesser Himalayan sediments (Searle 1986, Coward *et al.* 1986, Pecher & Le Fort 1986, Thakur 1987). The mechanisms of intraplate crustal shortening and internal deformation in the Higher Himalaya and along the MCT zone are locally understood in the Nepal Himalaya (Pecher 1977, Bouchez & Pecher 1981, Le Fort 1981, Brunel 1986, Pecher & Le Fort 1986). This paper aims mainly to document the strain patterns during the D_2 deformation phase in a NE-dipping 15–20 km wide intraplate ductile shear zone of the overthrust-type in a part of the NW Himalaya.

REGIONAL GEOLOGY AND DEFORMATION PATTERNS

Recent Rb–Sr whole-rock dates from the Higher Himalayan metamorphic rocks reveal the involvement of a Precambrian basement of 1800–2300 Ma in the Cenozoic Himalayan Orogeny (Bhanot *et al.* 1980, Trivedi *et al.* 1984, Singh *et al.* 1986). These basement rocks are thrust southwestward over predominantly late Proterozoic Lesser Himalayan sediments along the NE-dipping Main Central Thrust (MCT) and associated thrusts of regional dimensions (Fig. 1) (Heim & Gansser 1939, Thakur 1987). In parts of the Tons–Rupin–Supin Valleys of the Garhwal Himalaya, the Lesser Himalayan quartzite (Gamri Quartzite) of the Garhwal Group is separated from the Central Crystalline Zone of the Higher Himalaya by the MCT. The MCT is concealed beneath the imbricate Jutogh Thrust Sheet (Fig. 2) (Anand 1986). The Central Crystalline Zone is composed of two NE-dipping major lithotectonic groups whose lithological characteristics are summarized in Table 1.

Of the four deformational phases the earliest phase, D_1, is very rarely seen. It comprises rare appressed tight to isoclinal F_1 folds of 'flame-type' (Class IC → 2) on lithological banding with an axial-plane foliation S_1 (Fig. 3a). Early linear L_1 structures such as stretching/mineral lineations are seen rarely around F_2 fold hinges.

The second deformation (D_2) is most pervasive with the development of an intense planar fabric, S_2, a NE–SW-plunging mineral/stretching lineation, L_2, and F_2 folds (Fig. 4a and b). The S_2 foliation is axial-planar to close to isoclinal, reclined to recumbent, F_2 folds (Class 1C → 2) (Fig. 3b). A well-marked stretching/mineral lineation (L_2) on the composite foliation (S_1–S_2) is parallel to F_2 fold axes and is genetically related to the D_2

Table 1. Lithotectonic succession of the Central Crystalline Zone of the Higher Himalaya along the Tons–Rupin–Supin Valleys, NW Garhwal (Rb–Sr data after Singh *et al.* 1986)

	Tectonic units	Lithotectonic units	Lithology
Central Crystalline Zone	Jutogh Thrust Sheet	Jutogh Group	Harkidun granite–gneiss Fine-grained biotite schist, quartz-biotite gneiss Quartz–biotite–muscovite–kyanite–garnet gneiss and schist Quartz–muscovite–biotite–garnet schist and gneiss Banded gneiss Quartz–chlorite schist, mylonite gneiss Calc-schist and phyllite
		Jutogh Thrust	
		Imbricate zone	Imbricate of Gamri Quartzite and biotite gneiss (Naitwar Group)
		Main Central Thrust	
	Naitwar Crystalline Unit	Naitwar Group (1811 ± 133 Ma)	Chlorite schist, quartz–mica schist/gneiss Porphyroblastic gneiss, augen gneiss Amphibolite, mylonitized augen gneiss
		Main Central Thrust	
Lesser Himalaya		Garhwal Group (Gamri Quartzite)	Quartz–sericite schist Quartizite

ductile shearing deformation (Fig. 3c). In the schistose quartzite of the Garhwal Group, this lineation is defined by elongate porphyroclastic and recrystallized quartz and thin muscovite–sericite flakes. In the Central Crystalline Zone, inequant quartz and feldspar aggregates are streaked out along this dominant linear fabric as thin stretched lenses and ribbons in XZ sections both in gneiss and schist (Fig. 3d). In these rocks, elongate ribbons or trains of fine inequant recrystallized grains are parallel to the mineral alignment of biotite, muscovite and amphibole. Syntectonic garnet, staurolite and kyanite porphyroblasts were rotated sinistrally during the ductile shearing in D_2. Asymmetric pressure fringes around porphyroblasts and S–C relationships between fabrics of the S_2 foliation (Fig. 3e) predominantly support top to south ductile shearing (cf. Berthé *et al.* 1979).

F_2 folds and L_2 lineations maintain their consistent NE orientation irrespective of the attitude of the composite foliation and thrust zones containing them (Fig. 4a & b). The linear fabric represents the X direction of the strain ellipsoid in the direction of tectonic transport of thrust sheets in the Garhwal Himalaya (also, Coward *et al.* 1982, Brunel 1986).

The D_3 deformation phase is characterized by gently NW–SE plunging tight to isoclinal F_{3a} folds (Class 1B → 1C → 3) on the earlier foliations S_1–S_2. The axial-plane foliation (S_{3a}) of these folds cuts across the folded S_2 foliation in hinge zones of the F_{3a} folds with a moderate dip towards NE or SW (Figs. 3f and 4c). A faint mineral lineation of biotite–muscovite flakes parallel to F_{3a} fold hinges makes angles of 40–90° with the more intense L_2 lineation (Fig. 4d). Subsequently, F_{3b} folds of open to close and inclined type (Fig. 3f) with characteristic crenulation foliation (S_{3b}) (Fig. 4f) are developed on S_1, S_2 and S_{3a} foliations (Fig. 4e).

Kinks, brittle–ductile discrete shear zones and tension gashes are developed at high angles to the composite foliation during the D_4 deformational phase. This phase of post-collision tectonism is manifested in the faster uplift and cooling of the metamorphic pile as determined by fission track ages on apatite, transverse lineaments, earthquake-induced deformation of soft-sediments and present-day seismicity (Anand 1986, Anand & Jain, 1987).

STRAIN PATTERNS

Choice of strain markers and methodology

The Central Crystalline Zone and the Lesser Himalayan Gamri Quartzite abound in quartz-rich gneiss and quartzite where quartz varies from 75 to 90%. In the quartzite, inequant quartz clasts possess very distinct elongate measurable grain boundaries. Most of such grains reveal uniform to mildly undulose extinction (Fig. 3g). Reconnaissance measurements of quartz aggregate grains (Fig. 3h) in the XZ sections of gneiss across the Central Crystalline Zone indicated significant variations near the ductile tectonic boundaries. Hence, regional strain analysis was undertaken to delineate strain patterns of the D_2 deformation when most of quartz grains appear to have attained stable grain boundaries. Effects of earlier D_1 strain appear to be minimum due to its isolated presence and was not considered in the analysis.

Before undertaking detailed regional work on strain patterns, 10 samples of quartzite and gneiss from three tectonic units were studied using three orthogonal thin sections along XY, XZ and XZ planes in order to determine the most accurate, reproducible and expedient method. About 60–110 grains from enlarged photomicrographs were used for the comparative strain analysis by the R_f/ϕ method (Ramsay 1967, Dunnet 1969), long/short axis method (Ramsay 1967), centre-to-centre method (Ramsay 1967), 'nearest neighbour' centre-to-centre method (Fry 1979), shape factor grid method (Elliott 1970) and mean shape method (Lisle 1977). The X direction is taken parallel to the stretching lineation along which mica, quartz and feldspar are elongated ($X > Y > Z$). The results of comparative strain analyses were plotted on respective diagrams and tabulated (Anand 1986).

A comparison of different methods of strain analysis reveals a good correlation of strain ratio (R_s) values by the Fry and R_f/ϕ methods. Although rather time-consuming, the R_f/ϕ method has been used by a number of investigators for regional strain analyses (Kligfield *et al.* 1981, Davidson 1983, Odling 1984, Siddans *et al.* 1984).

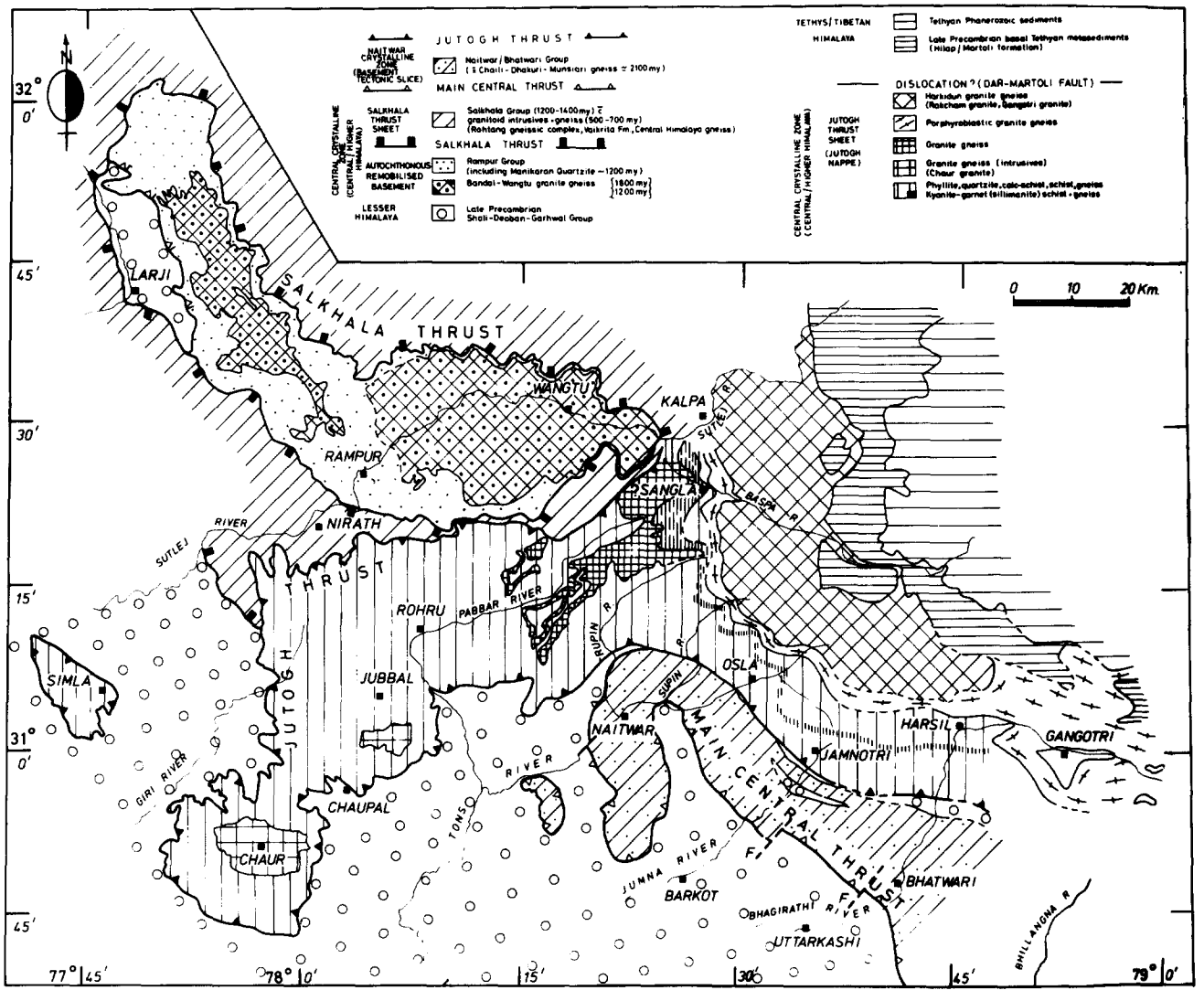

Fig. 1. Tectonic map of the Simla–Kinnaur region, Himachal Pradesh and NW Garhwal Himalaya (compiled and modified after Pilgrim & West 1928, Tewari *et al.* 1978, Bhargava 1980).

For the present strain analysis, it was assumed that quartz grains originally approximated to randomly oriented ellipsoids in shape having negligible ductility contrast with the matrix during homogeneous strain. For the first assumption, an indirect check is available on specimens by 'nearest neighbour' centre-to-centre methods by Fry (1979) and Ramsay (1967). Plots by the Fry method on all samples show a parallelism between the strain ellipse and macroscopic deformation axes. High goodness of correlation of ellipses indicates an initial random uniform distribution and homogeneous deformation on the scale of the thin section.

For the second assumption on negligible ductility contrast, analysed specimens of quartzite are mostly composed of quartz, and therefore bear minimum compositional heterogeneity. In gneiss, selective portions of thin sections having maximum proportion of quartz to matrix were chosen for the strain analysis to minimize ductility contrast.

Measurements of R_f/ϕ data on three mutually perpendicular principal planes are generally made, although only two sections are required to determine the three principal strain ratios. The third section provides an independent check on the accuracy of results because $R_s(XZ) = R_s(XY)$. $R_s(YZ)$ (Dunnet 1969, Ramsay & Huber 1983) and may record an error up to 5% in some samples. The validity of this relationship was checked on samples from the Gamri Quartzite (Anand 1986). A combination of logarithmic mean of R_f maximum and R_f minimum with the onion curves given by Dunnet (1969) was used in the determination of R_s values. As the determined R_s values were found to vary systematically, it appears that inherent errors in the method were insignificant compared to the actual differences. A cross-check was made by the Fry (1979) method. The three-dimensional strain data were plotted (Anand 1986) on Flinn, logarithmic and Hsü graphs (Flinn 1956, 1962, Hsü 1966, Ramsay 1967, Ramsay & Huber 1983). Only the Hsü plots are reproduced here.

REGIONAL STRAIN PATTERNS

Strain variation in the Garhwal Group

Twenty-three oriented samples from the Gamri Quartzite of the Garhwal Group were selected for the

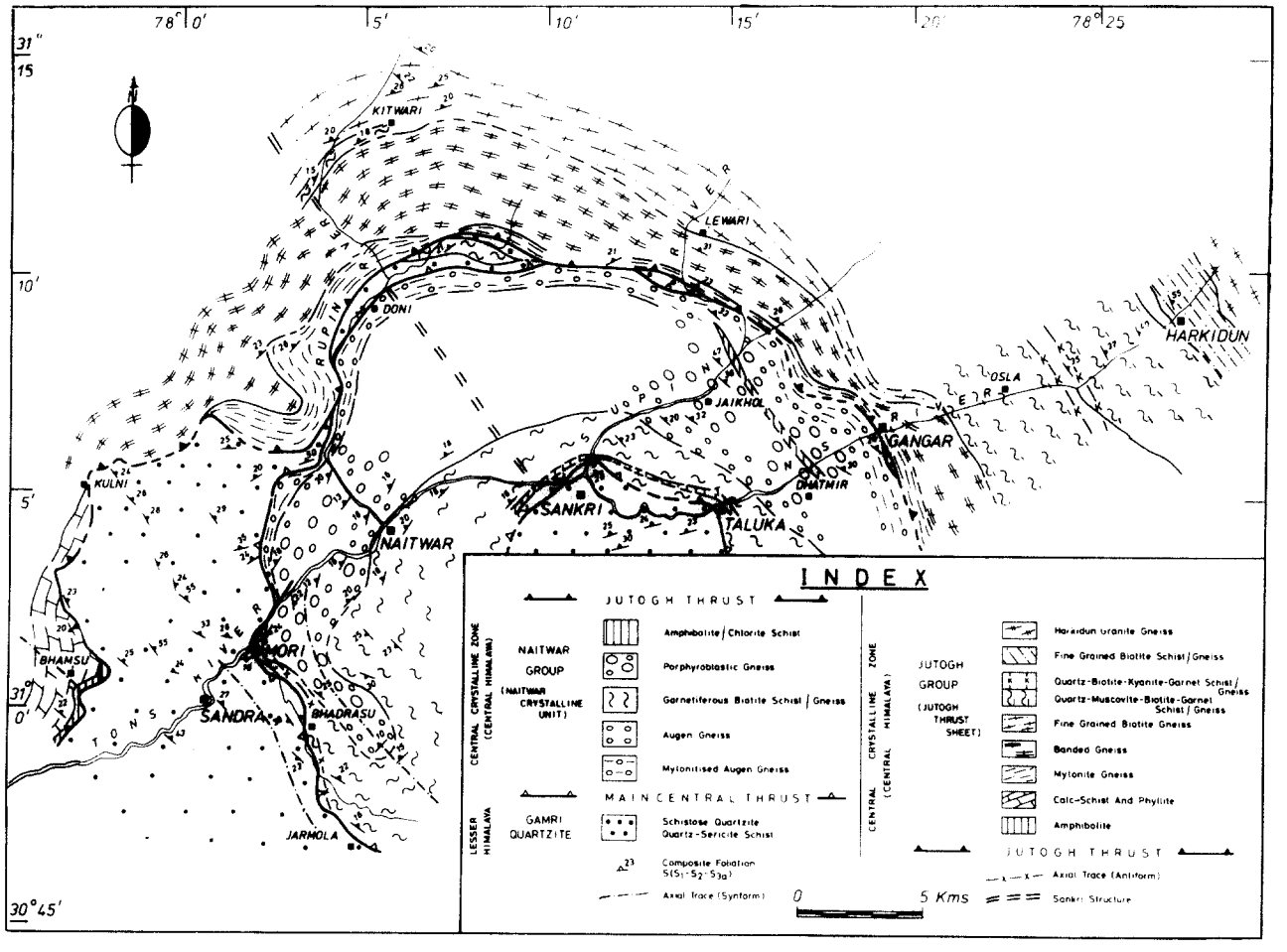

Fig. 2. Geological map of the Garhwal Group and the Central Crystalline Zone along the Tons–Supin–Rupin Valleys, NW Garhwal.

strain analysis. Twenty of the samples are systematically distributed around Sankri (Fig. 5), while three are from the Sandra-Mori section to the south on the subthrust side of the MCT. All R_f/ϕ curves show that the bulk of the measured grains plot symmetrically about the principal strain axis and correspond to the predicted field of homogeneous deformation. The lack of points around the centre of the XY plot indicates an absence of initially circular particles (cf. Dunnet 1969).

The XZ sections of quartzite specimens from the Garhwal Group show high values of strain in the vicinity of the Main Central Thrust (MCT) zone from $R_s = 1.89$ to 2.16 with an initial axial ratio R_i from 1.37 to 1.94 (Anand 1986). Away from the MCT around Sankri area, specimens show low values of strain with R_s ranging from 1.52 to 1.62 southwestwards, while R_i varies from 1.28 to 1.78. A high strain zone is again encountered further southwestward in a structurally lower traversed road section, where the R_s value increases to 2.00 with R_i reaching 1.80 (Sample A15).

Two-dimensional R_f/ϕ finite strain data from all the quartzite samples are integrated for three-dimensional strain analysis to determine the shape of strain ellipsoid and values of different strain parameters (i.e. k, K, ν and $\bar{\varepsilon}_s$; Anand 1986). On the Flinn graph and logarithmic strain plot, all data points lie in the flattening field. k values increase from 0.36 to 0.82 and approach the field of plane strain (assuming constant volume) near the basal part of the MCT. A contoured map of k values reveals an increase in its values in a lensoid-shaped high-strain zone within the Garhwal Group (Fig. 6). Low k values (0.27) are also found in the immediate vicinity of the MCT. In the lower tectonic section, k values again increase to more than 0.60.

Calculated $\bar{\varepsilon}_s$ and ν values represented on a Hsü diagram indicate an average $\bar{\varepsilon}_s$ value of 0.38 in the field of flattening for a range of $\bar{\varepsilon}_s$ values of 0.3 to about 0.6 (Fig. 7a). Contours of strain magnitude, $\bar{\varepsilon}_s$, trend nearly SE subparallel to the surface trace of the MCT (Fig. 7b), although in places cut by the thrusts and oblique to the ENE-striking S_2 foliation in the quartzite. $\bar{\varepsilon}_s$ values greater than 0.55 are found near the MCT and gradually decrease within the quartzite with increasing distance from the MCT across Sankri. Further south of a comparatively low strain zone, a second region of higher $\bar{\varepsilon}_s$ value (>0.45) occurs within the monotonous Gamri Quartzite. A contoured map of Lode's parameter (ν) shows that the shape fabric of the strain ellipsoids lies in the flattening field. In general, these values are lower near the tectonic boundaries (Fig. 7c).

This zone is, however, difficult to identify in the field due to the monotonous arenaceous lithology of the Gamri Quartzite. It is inferred that the high strain zone observed within the lower traversed portion of the

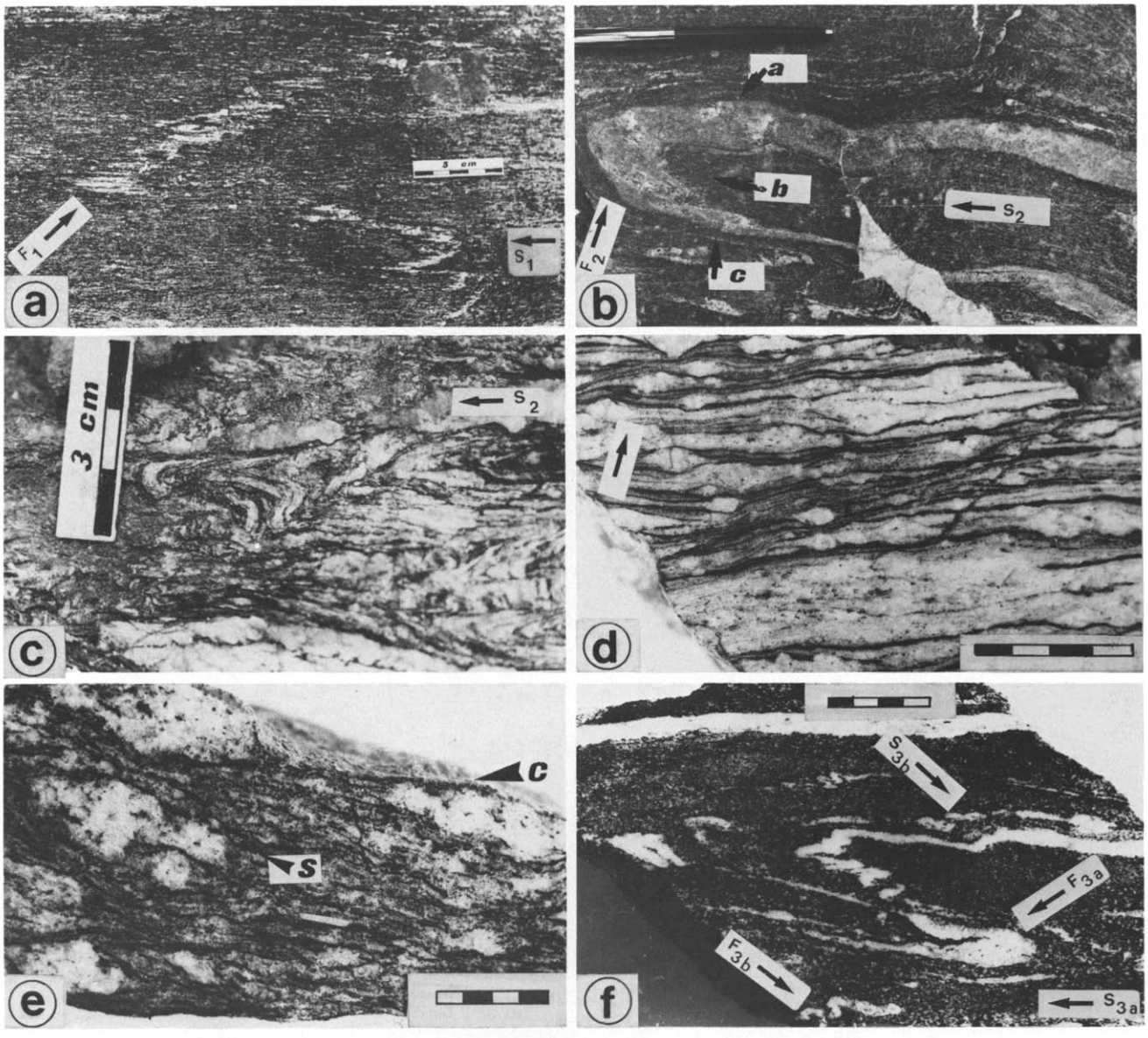

Fig. 3. Deformational structures from the Higher Himalayan metamorphics of the Tons–Rupin–Supin Valleys. (a) Tightly appressed F_1 isoclinal 'flame folds' in biotite gneiss and axial plane foliation S_1 of the D_1 deformational phase affecting quartz veins. Locality—1 km of Taluka. (b) Isoclinally folded S_1 gneissosity/foliation by F_2 folds of D_2 deformational phase in biotite gneiss. S_2 foliation parallels S_1 on the limbs but is at high angles in the hinge zone. Note change of asymmetry from S to Z on different limbs (labelled a and c) while Σ marks the hinge zone (labelled b). Locality–Taluka; pen 12 cm. (c) Discrete ductile shear zones parallel to S_2 axial plane foliation in F_2 folds of biotite gneiss. Locality—Osla. (d) Stretched quartz and feldspar porphyroclasts in XZ section parallel to the L_2 lineation. Discrete shear zones at low angles to S_2 foliation (arrow). Locality—Naitwar; scale 2 cm. (e) S and C composite planar fabric of the S_2 foliation showing asymmetrical feldspar augen and sigmoidal bending of S plane along C (ductile shear) surfaces with sinistral vergence. Locality—Taluka; scale 2 cm. (f) Profile of F_{3a} isoclinal to tight folds of D_3 deformational phase with transposition of limbs along S_{3a} foliation. Coaxial F_{3b} folds are superposed on long limbs in garnet–biotite gneiss. Locality—Harkidun; scale 2 cm (*continued*).

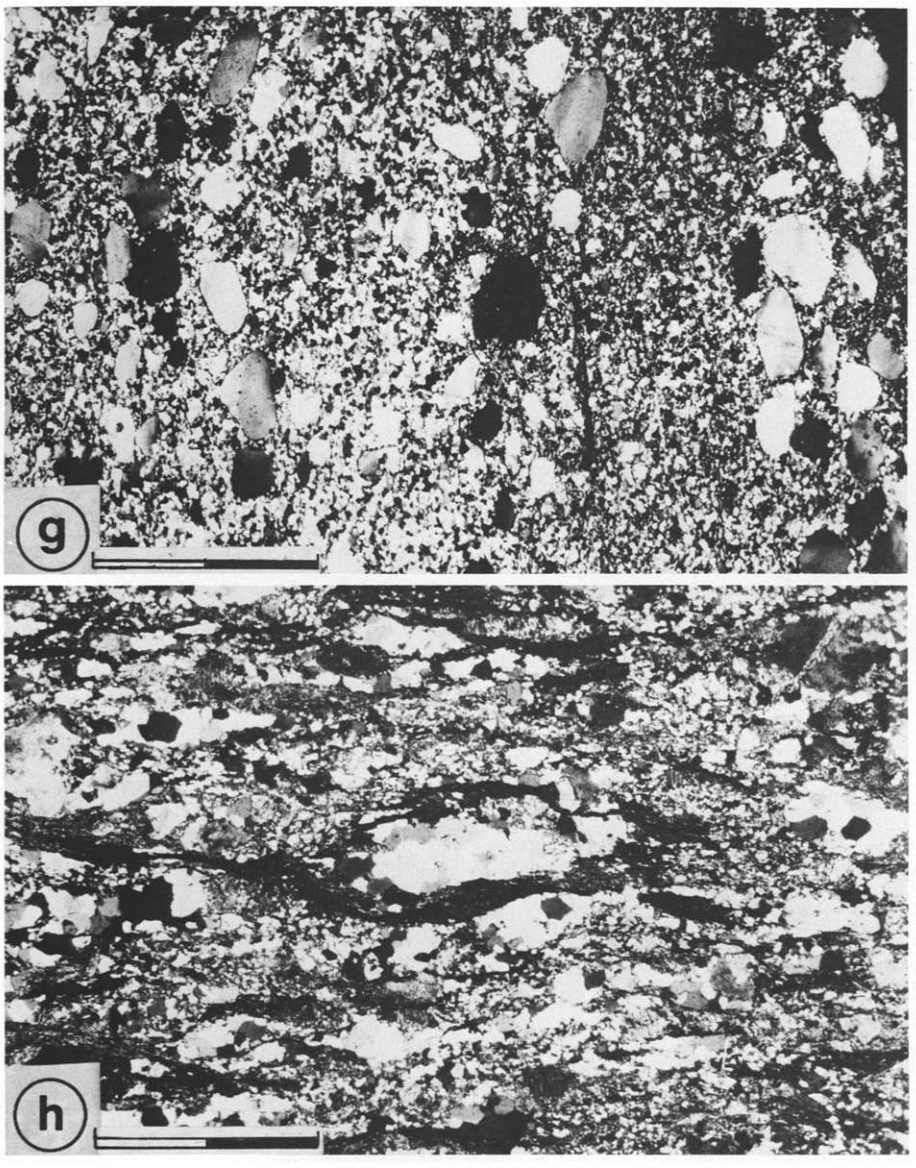

Fig. 3. (*continued*) (g) Photomicrograph of deformed detrital quartz as strain marker in *YZ* section of Gamri Quartzite (Lesser Himalaya). Locality—Sandra; scale 2 mm. (h) Recrystallized quartz aggregate used as strain marker in *XZ* section from gneiss (A80) of the Higher Himalayan metamorphics. Locality—SW of Doni; scale 2 mm.

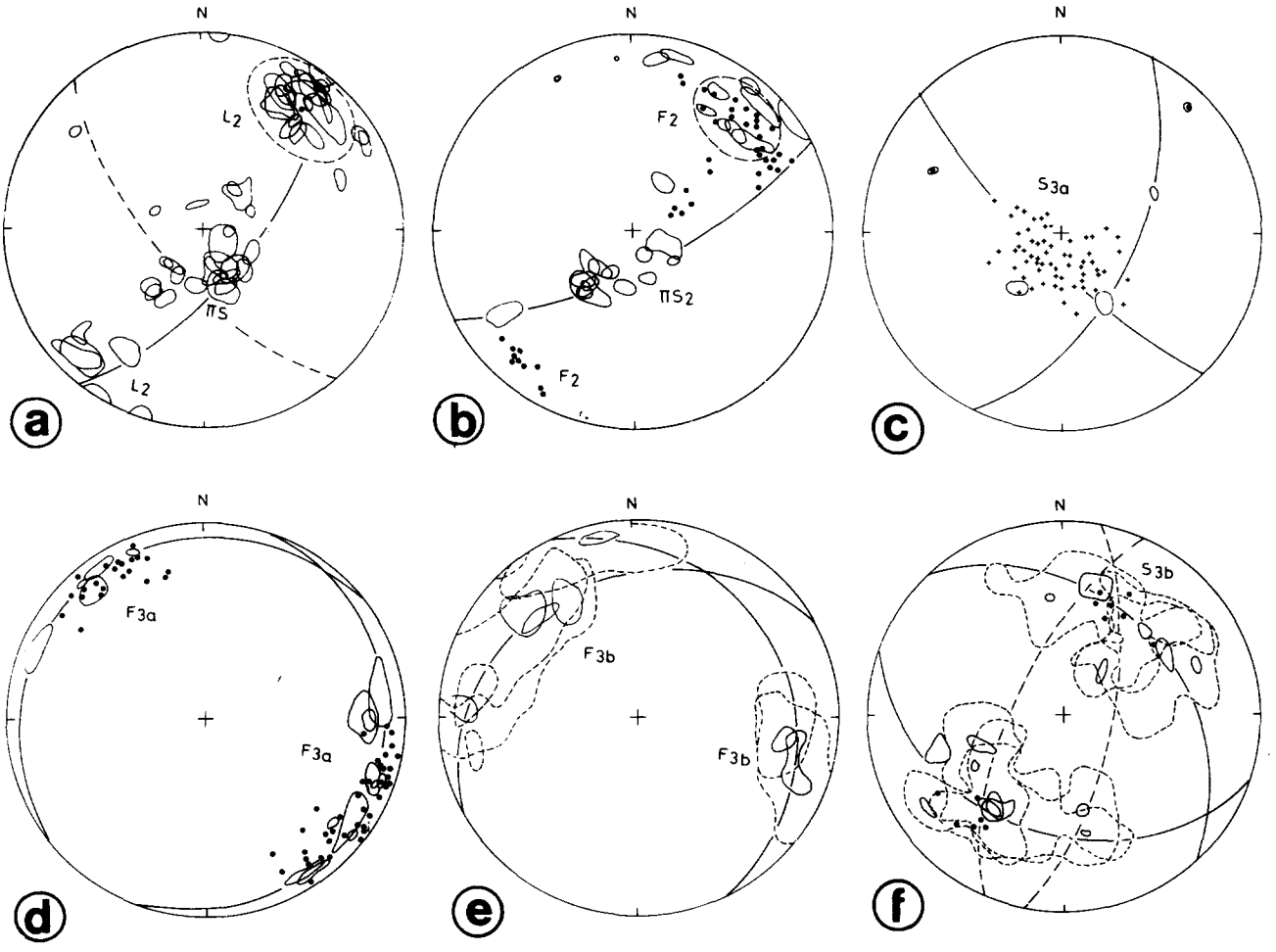

Fig. 4. Orientation data from the Lesser Himalayan quartzite and Higher Himalayan metamorphics of the Tons–Supin–Rupin Valleys, Garhwal, from 25 domains. (a) π-diagram of composite S_1 and S_2 foliation (n = 957) containing L_2 lineation (n = 1130). (b) π-diagram of S_2 foliation (n = 881) with F_2 fold axes (n = 501). (c) π-diagram of S_{3a} foliation (n = 184). (d) F_{3a} fold axes (n = 416). (e) F_{3b} fold axes (n = 181). (f) π-diagram of S_{3b} foliation (n = 242). Solid contours represent maxima from individual domains; dashed contours indicate outermost contour. Dots and plus are scatter data in some individual domains.

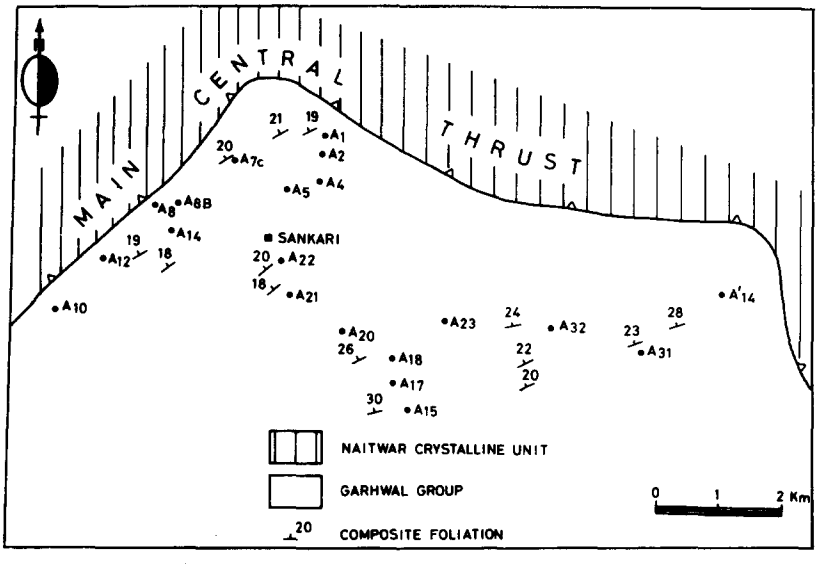

Fig. 5. Location map of samples for strain analysis from the Lesser Himalayan Gamri Quartzite around Sankri.

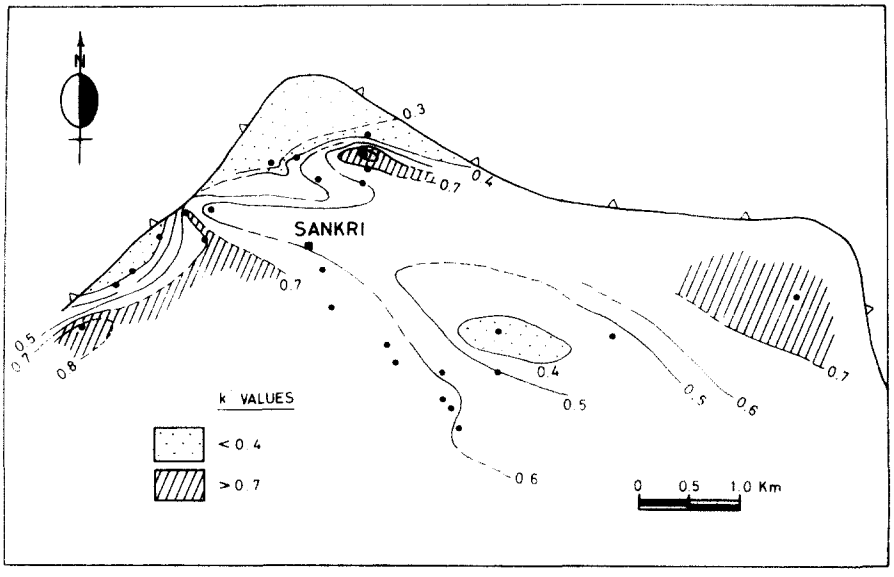

Fig. 6. Spatial variation in k values of the Gamri Quartzite around Sankri:

$$k = \frac{R_{xy} - 1}{R_{yz} - 1} = \frac{a - 1}{b - 1} = \frac{(1 + e_3)(e_1 - e_2)}{(1 + e_2)(e_2 - e_3)}$$ (Flinn 1956, Ramsay 1967).

Gamri Quartzite represents another late D_2 ductile shear zone. Another thrust has probably evolved and tectonically transported this high strain zone to the surface either as an imbricate zone of the MCT or a new tectonic dislocation.

Strain variation in the Central Crystalline Zone

Thirty-eight samples of gneiss from the Naitwar and Jutogh Groups of the Higher Himalaya were analysed from the XZ and YZ sections of each sample (Fig. 8). Finite strain in two dimensions from XZ sections of all specimens indicate a very consistent pattern of strain ratios in all three valleys at approximately the same structural level. Near the basal parts of two thrusts (the MCT and the Jutogh Thrust), XZ sections of gneiss reveal higher strain ratios of $R_s = 2.0$–2.13 with a range of R_i values from 1.64 to 1.74. In the basal gneiss of the Naitwar Group, XZ sections show strain ratios ranging from 1.79 to 2.13 near the MCT. Moving up the thrust pile, the R_s values decrease to a minimum of 1.64 and the R_i value is 1.54. Northward near the Jutogh Thrust, the R_s values again increase to a maximum of 2.14, with $R_i = 1.60$. Identical trends in R_s values are seen in the Jutogh Group where minimum values characterize the middle part of the sequence. R_s values increase both towards the base near the Jutogh Thrust and upwards near the contact with the Harkidun granite gneiss, where $R_s = 2.13$ and $R_i = 1.49$.

The Flinn and logarithmic plots of k and K values show that finite strain in the metamorphic rocks is of flattening type. However, near the major tectonic boundaries (the Main Central Thrust, the Jutogh Thrust and near the Harkidun granite gneiss body) higher k values of up to 0.90 have been recorded signifying strain ellipsoids close to plane strain (Anand 1986).

The spatial variation in k values in the Central Crystalline Zone indicates a zone of low k nearly in the middle of each tectonic unit followed by a gradual increase towards the tectonic boundaries (Fig. 9). Near the MCT and the Jutogh Thrust, k values are more than 0.5 and sometimes approach 0.85. Near the Jutogh Thrust, a discontinuity in k values is noticeable. Near the Harkidun granite gneiss k values reach a maximum of 0.88 which is approaching plane strain.

In the Hsü three-axis polar diagram, $\bar{\varepsilon}_s$ and ν values of all the gneiss samples indicate a distinct field of flattening with maximum $\bar{\varepsilon}_s = 0.534$ near the Harkidun granite gneiss (Fig. 10a). Spatial variations of $\bar{\varepsilon}_s$ and ν clearly demarcate zones of high strain magnitude and low strain symmetry near the major tectonic boundaries (Fig. 10b & c). These tectonic zones are characterized by $\bar{\varepsilon}_s$ values of more than 0.5 (Fig. 10b). In the western parts of the MCT and the Jotogh Thrust, $\bar{\varepsilon}_s$ and ν contours are truncated by these dislocations.

The relationship of the strain parameters to the distance from the main tectonic boundaries clearly indicate discontinuities in the strain in each zone which are different for the three valleys (Fig. 11a–c). In the Naitwar Group, high values of k, K and $\bar{\varepsilon}_s$ characterize both the MCT and the Jutogh Thrust. The values decrease to a minimum before increasing again towards the Jutogh Thrust. In the Tons Valley, the strain discontinuity characterizing the Jutogh Thrust (Fig. 11a) is less severe than for the Supin (Fig. 11b) and Rupin (Fig. 11c) Valleys. The strain parameters (k, K and $\bar{\varepsilon}_s$) again attain maximum values near the Harkidun granite gneiss, representing a zone of high strain (Fig. 11a). This pattern of strain parameters seems, therefore, to be characteristic of ductile shear zones in the Higher Himalaya.

SPATIAL STRAIN VARIATIONS

In the Higher Himalaya, all the three tectonic boundaries demarcated by the MCT, the Jutogh Thrust and the

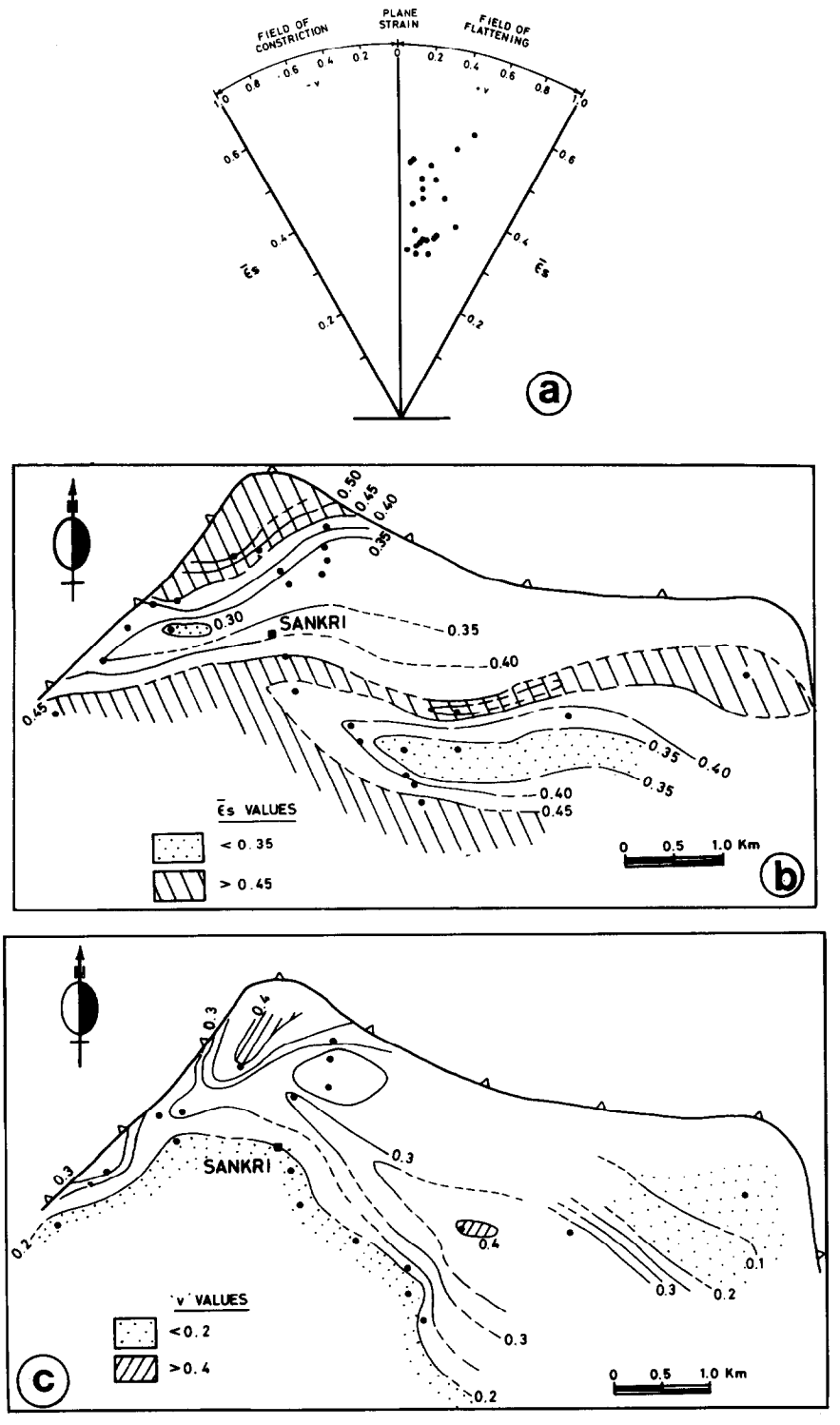

Fig. 7. (a) $\bar{\varepsilon}_s$ vs ν polar graph for the Gamri Quartzite beneath the MCT around Sankri. (b) Spatial variation in $\bar{\varepsilon}_s$ values of the Gamri Quartzite. (c) Spatial variation in ν values of the Gamri Quartzite, where

$$\nu = \frac{2\,\varepsilon_2 - \varepsilon_1 - \varepsilon_3}{\varepsilon_1 - \varepsilon_3} = \frac{(\varepsilon_2 - \varepsilon_3) - (\varepsilon_1 - \varepsilon_2)}{(\varepsilon_2 - \varepsilon_3) + (\varepsilon_1 - \varepsilon_2)} \quad \text{(Hossack 1968).}$$

$$\bar{\varepsilon}_s = \frac{\sqrt{3}}{2}\gamma_{oct} \quad \text{(Nadia 1963), where octahedral unit shear}$$

$$\gamma_{oct} = \tfrac{2}{3}[(\varepsilon_1 - \varepsilon_2)^2 + (\varepsilon_2 - \varepsilon_3)^2 + (\varepsilon_3 - \varepsilon_1)^2]^{1/2} \quad \text{(Nadia 1963)}$$

or

$$\bar{\varepsilon}_s = \frac{1}{\sqrt{3}}[\ln R_{xy}^2 + \ln R_{yz}^2 + \ln R_{xz}^2]^{1/2} \quad \text{(Ramsay \& Huber 1983).}$$

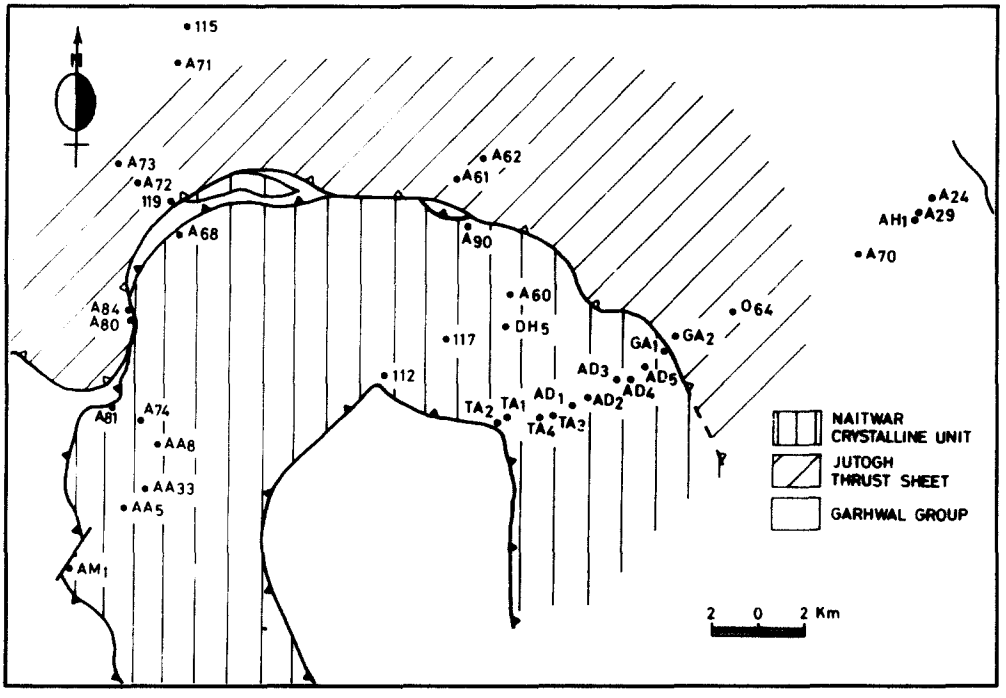

Fig. 8. Location map of gneiss samples for strain analysis of the Central Crystalline Zone.

Harkidun granite gneiss are marked by high K and $\bar{\varepsilon}_s$ values which approach the field of plane strain in the Tons, Supin and Rubin Valleys. In the Naitwar Group, for example, as one approaches the MCT from the middle, K values gradually increase from 0.18 to 0.59. Similarly, there is an increase in K values from 0.45 to 0.90 towards the Harkidum granite gneiss where the shape of the strain ellipsoid approaches plane strain.

Spatial variations in strain values defined by ν and $\bar{\varepsilon}_s$ values of the gneissic rocks from the Central Crystalline Zone are shown on Hsü three-axis diagrams (Fig. 12). The $\bar{\varepsilon}_s$ values gradually increase from 0.44 in the middle to 0.505 near the MCT and are represented by curved lines. Likewise, near the Harkidun granite gneiss body in the Tons Valley, high $\bar{\varepsilon}_s$ values ($\simeq$0.534) are encountered (Fig. 12a), but away from it at a distance of about 8 km southwestward, $\bar{\varepsilon}_s$ = 0.46. Identical patterns characterize the Supin and Rupin Valleys (Fig. 12b & c).

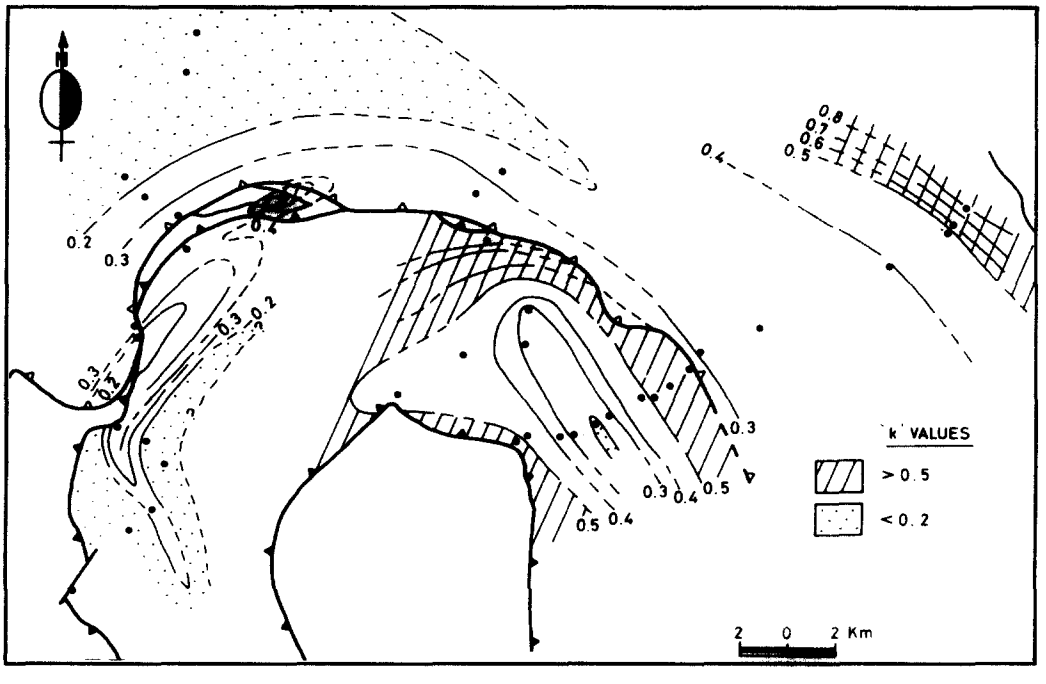

Fig. 9. Spatial variation in k values from the Central Crystalline Zone.

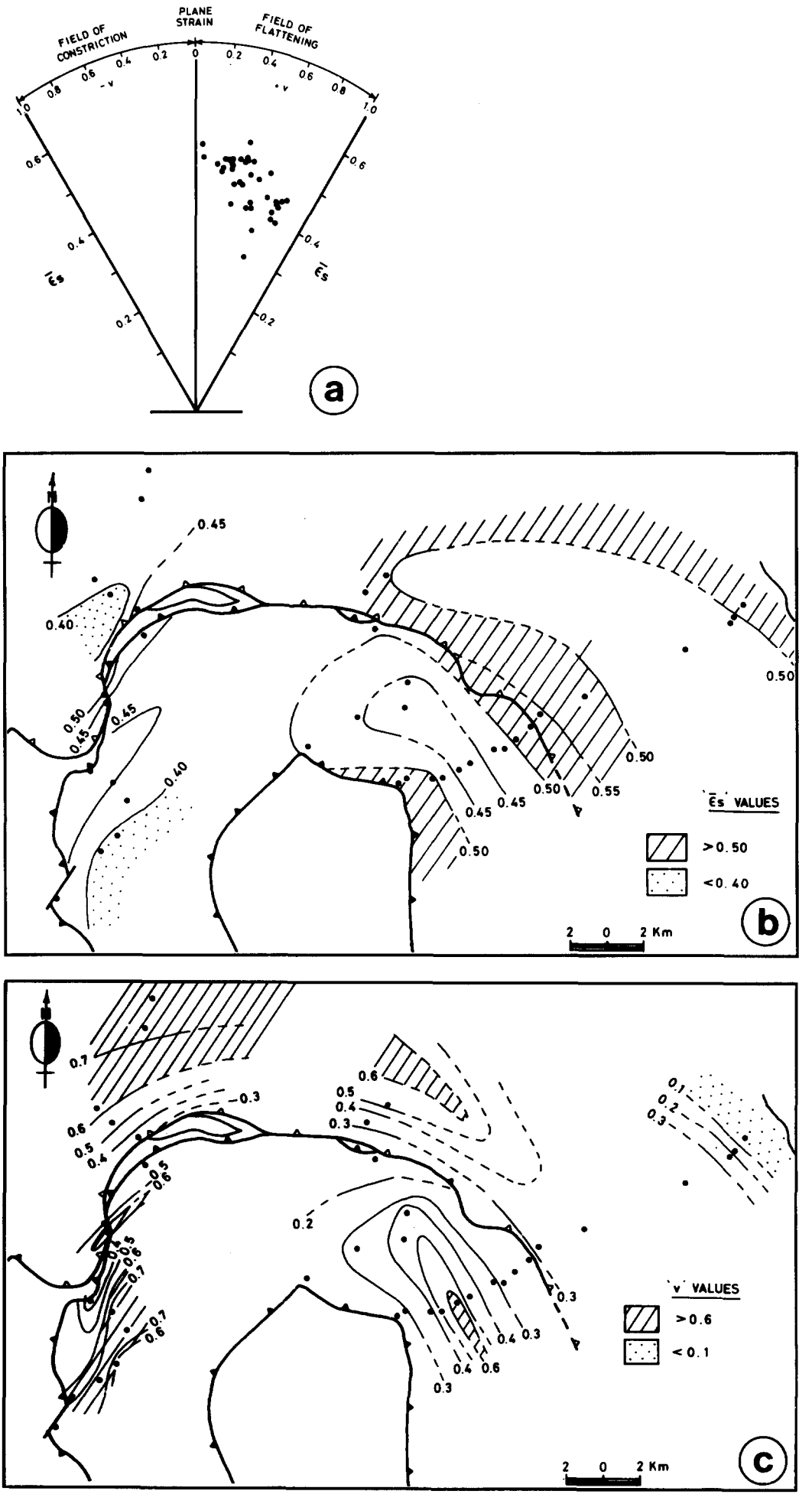

Fig. 10. (a) $\bar{\varepsilon}_s$ vs ν polar graph for the Central Crystalline Zone. (b) Spatial variation in $\bar{\varepsilon}_s$ values. (c) Spatial variation in ν vaues. Variables as in Fig. 7 caption.

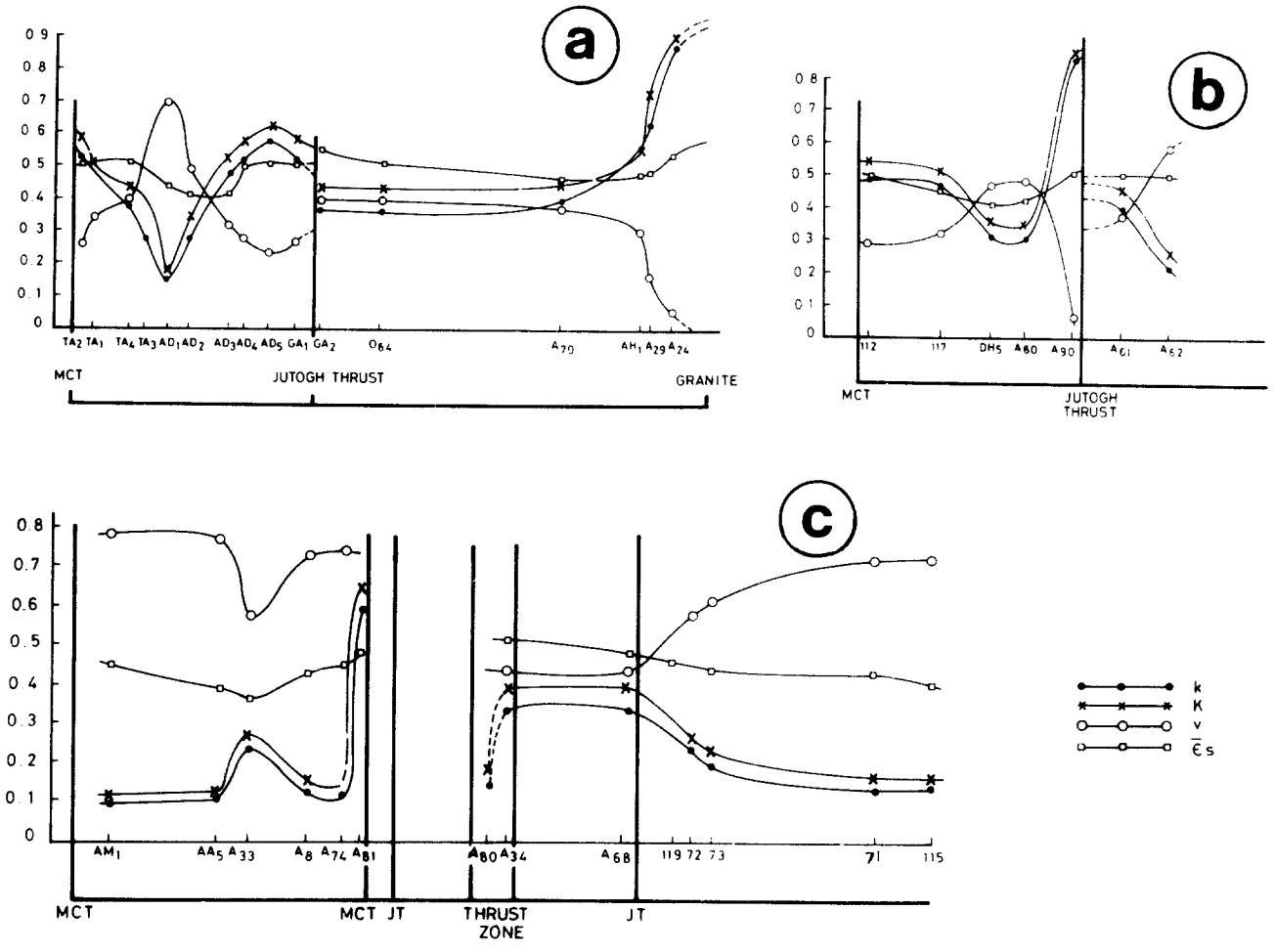

Fig. 11. Variation of different strain parameters in the Central Crystalline Zone along various cross-sections. (a) The Tons Valley. (b) The Supin Valley. (c) The Rupin Valley.

STRAIN AND ORIENTATION OF STRAIN ELLIPSOIDS

Strain maps and spatial orientation of strain ellipsoids in XZ and XY planes for both the Gamri Quartzite near Sankri (Fig. 13) and the Central Crystalline Zone (Fig. 14) reveal a consistent NE-trend of the X axis of the strain ellipsoid parallel to the stretching/mineral lineation L_2 in both the tectonic units of the Garhwal Himalaya. This trend persists almost across the quartzite of the Lesser Himalaya, the Naitwar Crystalline Unit and the Jutogh Thrust Sheet and is not deflected either in the thrust zones or in the regions of the Rupin–Tons Valleys, where the NW–SE-trending XY plane of the strain ellipsoid undergoes progressive rotation towards NE–SW.

Data on the stretching lineation L_2 parallel to X and foliation S_2 parallel to the XY plane of the strain ellipsoid for the Gamri Quartzite indicate that X consistently plunges NE at very low angles, while Y plunges NW near Sankri (Fig. 15). In the Rupin Valley, the Naitwar Crystalline Unit and the Jutogh Thrust Sheet are characterized by a NE-plunging X axis and generally NW-plunging Y axis (Fig. 16a). The orientation of the Z axis gradually changes to a steeply SW-plunging axis in the Naitwar and the Jutogh Groups of the Tons-Supin Valleys (Fig. 16a–c).

INTRACONTINENTAL CRUSTAL SHORTENING—A MODEL FOR CONTINENT–CONTINENT COLLISION

The Himalayan Mountain arc is characterized by immense intracontinental crustal shortening resulting from the collision of two continental margins (Gansser 1964). This produced the Higher Himalayan metamorphic belt and several major shear zones of which the MCT and associated thrusts are the classic examples (Bouchez & Pecher, 1981, Brunel 1986, Mattauer 1986). Various tectonic models have been proposed for such intracontinental ductile shear zones which may either be transcurrent shear zones with considerable horizontal strike-slip movements (Berthé *et al.* 1979, Ramsay & Allison 1979, Brun & Pons 1981, Choukroune & Gapais 1983, Boullier 1986, Takagi 1986) or gently-dipping shear zones of the overthrust type (Carmignani *et al.* 1978, Kligfield 1979, Bouchez & Pecher 1981, Kligfield *et al.* 1981, Burg *et al.* 1984, Brunel 1986, Mattauer 1986, Platt & Behrmann 1986).

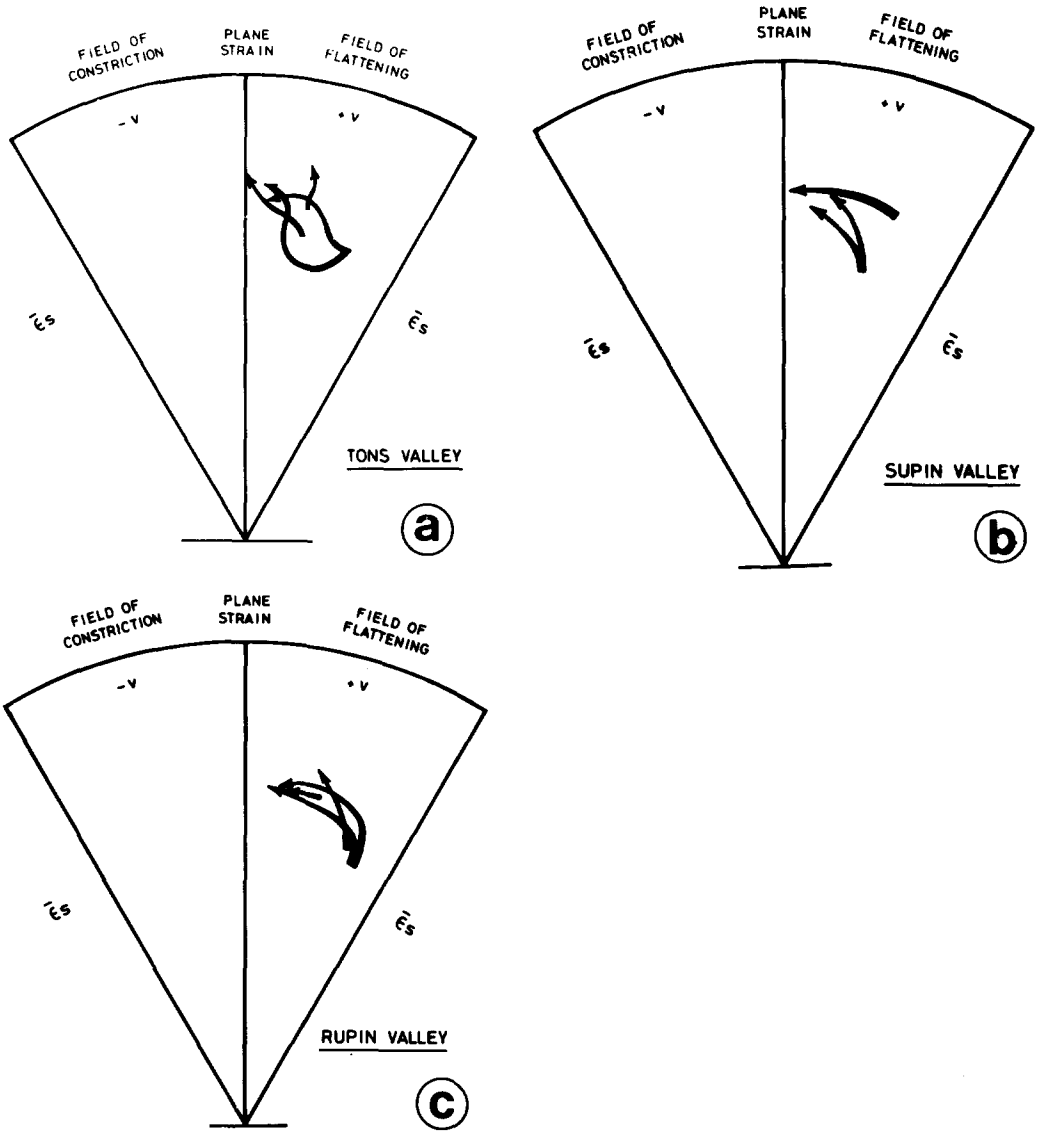

Fig. 12. Spatial strain variation of the Central Crystalline Zone on Hsü diagrams for the three valleys. (a) Tons Valley, (b) Supin Valley and (c) Rupin Valley.

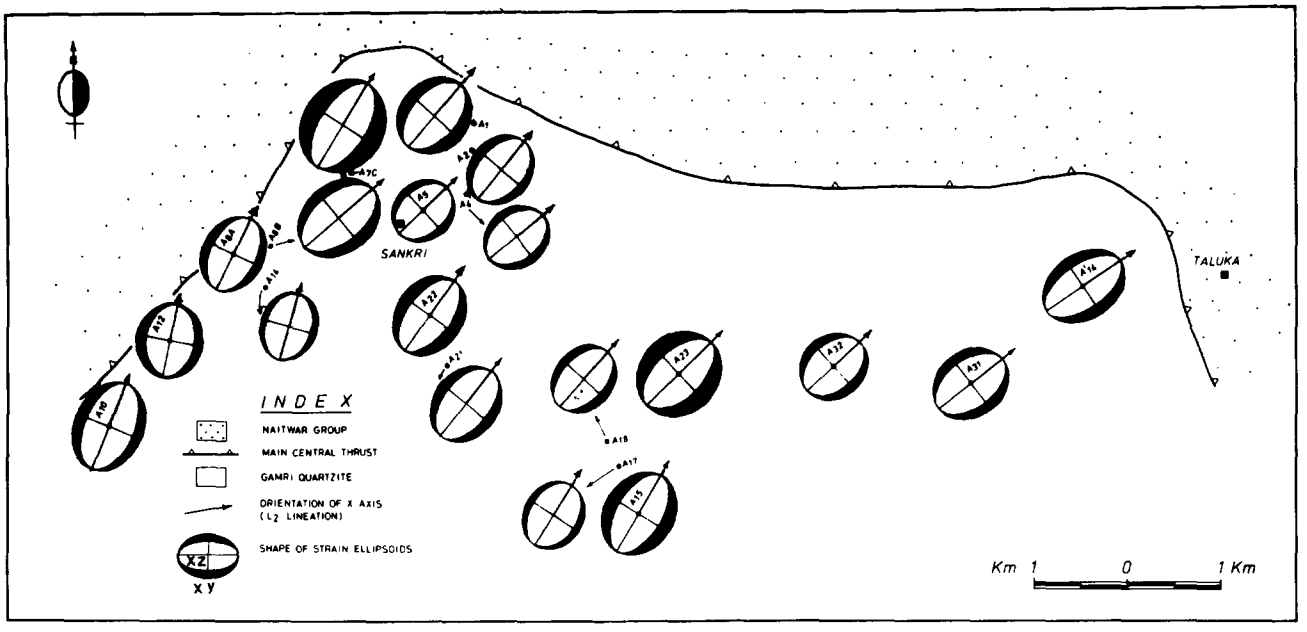

Fig. 13. Strain map of the Gamri Quartzite showing orientation of strain ellipse (XZ and XY) sections around Sankri.

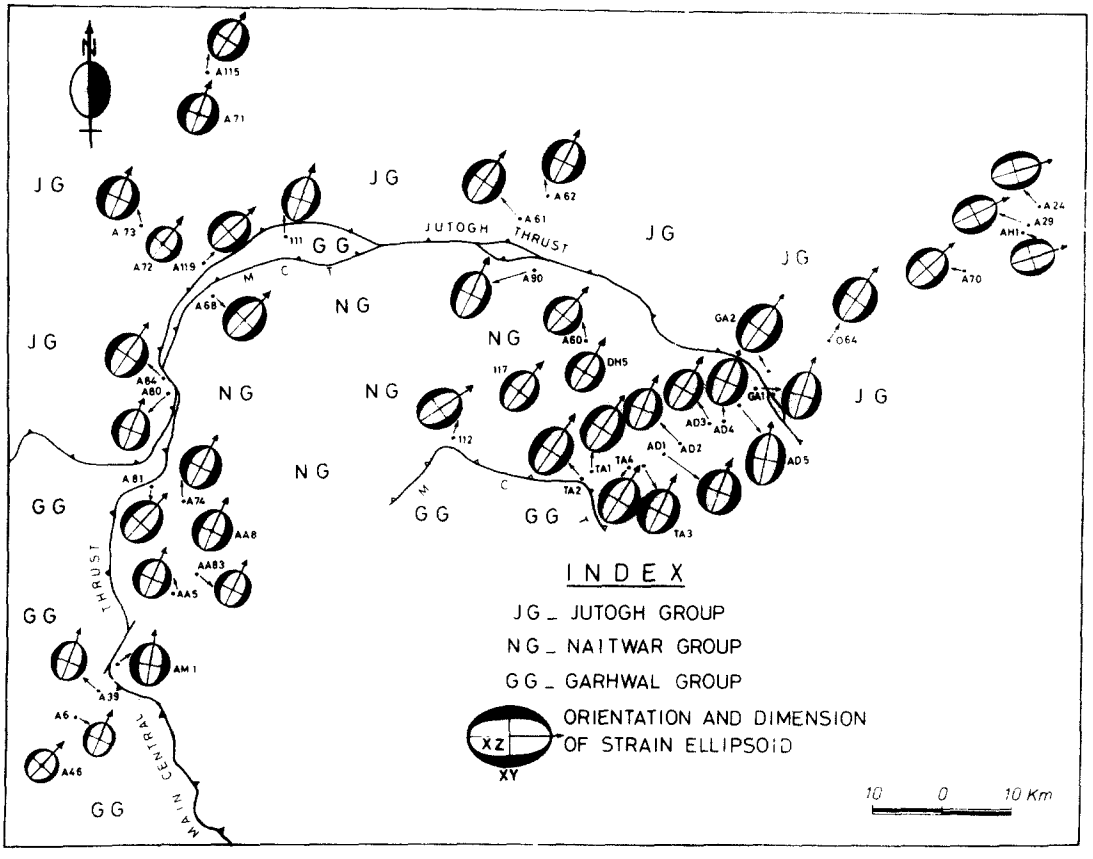

Fig. 14. Strain map of the Central Crystalline Zone showing orientation of strain ellipse (XZ and XY) sections from Tons–Supin–Rupin Valleys.

In the Higher Himalaya of the Central Crystalline Zone, the main penetrative S_2 foliation bears a well developed stretching lineation developed during the second deformational phase. A few occurrences of isolated F_1 folds depict their coaxial nature with later F_2 folds. Carmignani *et al.* (1978) proposed passive rotation of earlier folds into the extension direction during simple shear (Sanderson 1973, Escher & Watterson 1974, Rhodes & Gayere 1977, Williams 1978). Although a shear mechanism may have reoriented the earlier F_1 folds towards coaxial later F_2 folds, contemporaneous development of ubiquitous NE-plunging F_2 folds and L_2 stretching/mineral lineation with displacement in the broad ductile shear zone of the Central Crystalline pile is envisaged during the D_2 deformational phase (Fig. 17). Such a model would also explain the rotation of the earlier fabric towards the direction of maximum extension in thrust zones within the Himalaya and southern Tibet (cf. Bouchez & Pecher 1981, Burg *et al.* 1984), and is pertinent to the controversy regarding the presence of pre-Tertiary NE-trending structural elements in the Himalaya.

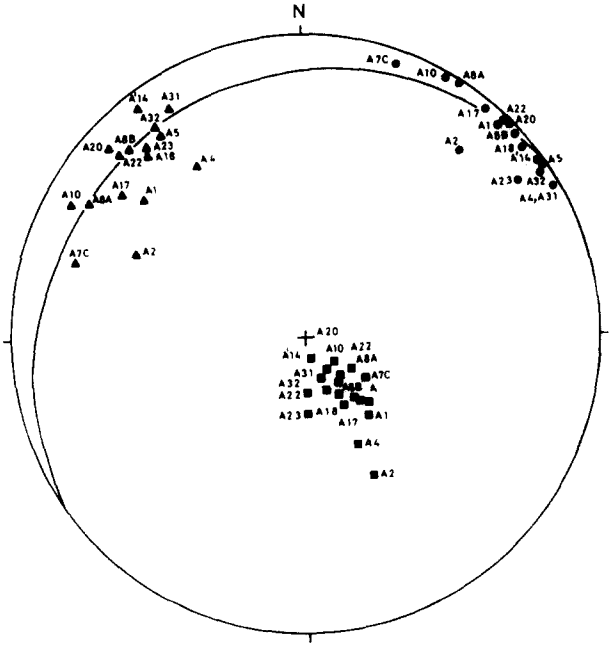

Fig. 15. Orientation of X (circle), Y (triangle) and Z (rectangle) axes of the strain ellipsoids in the Gamri Quartzite (Garhwal Group) along the Tons Valley around Sankri.

F_2 folds and L_2 lineations maintain their consistent orientation irrespective of the attitude of the composite foliation containing them (Fig. 17) and probably represent the X direction of the strain ellipsoid in the direction of tectonic transport of thrust sheets in the region. Since F_2 folds and associated stretching lineations L_2 have the same NE-trend in the whole metamorphic pile, continuity of direction indicates insignificant changes in kinematic directions during the deformation of Central Crystalline Zone and its subsequent translation. The composite S–C planar character of the S_2 foliation, rotation of porphyroblasts and pressure shadows all point towards SW-verging ductile shear movement in

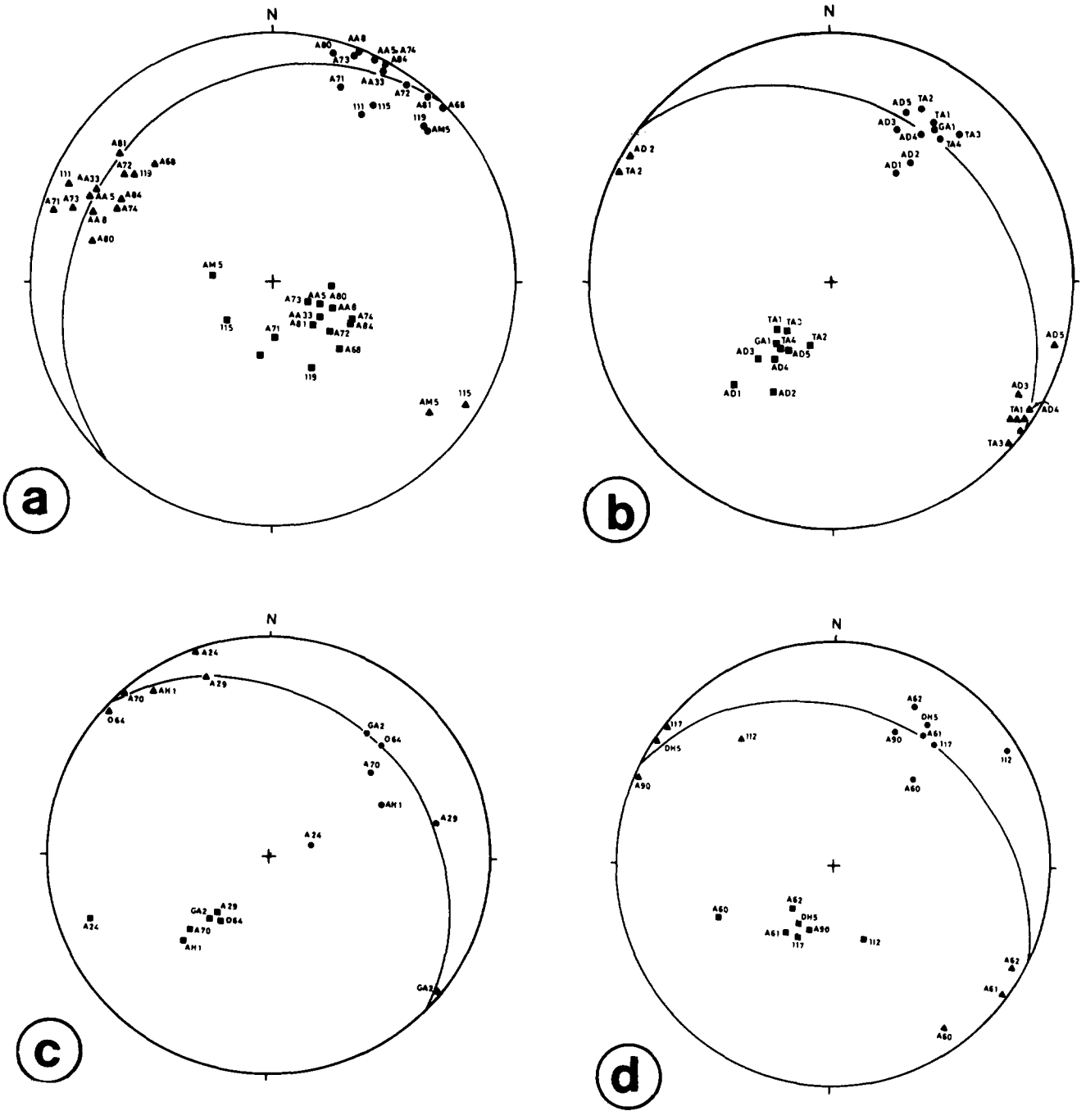

Fig. 16. Orientation of X, Y, Z axes of the strain ellipsoids. (a) The Central Crystalline Zone along the Rupin Valley and between Mori–Naitwar along the Tons Valley. (b) The Naitwar Group of the Tons Valley between Taluka and Gangar. (c) The Jutogh Group of the Tons Valley. (d) The Central Crystalline Zone in Supin Valley. Symbols for orientation of X, Y and Z axes as in Fig. 15.

the broad ductile shear zone of the rocks of the Central Crystalline Zone during the D_2 deformational phase. In the later part of the structural evolution with the development of F_{3a}, F_{3b} and F_4 folds whose axes trend at high angles to the F_2 folds, compression and brittle–ductile shear regime characterize the Central Crystalline Zone.

Regional strain variation in the Central Crystalline Zone clearly indicates the geometry of a broad ductile shear zone during the D_2 deformation. R_s values determined by R_f/ϕ techniques on quartz aggregates in the XZ sections of gneiss increase up to 2.2 both towards the base of the Naitwar Group near the MCT and towards the top near the vicinity of the Jutogh Thrust from a zone of low R_s values in the middle. Identical strain variations are observed in the Jutogh Group where low R_s values in the middle increase both towards the base of the Jutogh Crystalline unit and upwards near the contact with the Harkidun granite gneiss. k and K values of the finite strain ellipsoid lie in the field of flattening strain (see also Bouchez & Pecher 1981). Contoured maps of different strain parameters reveal the spatial variations in the k and K values within the Central Crystalline zones with maximum values near the main dislocation boundaries.

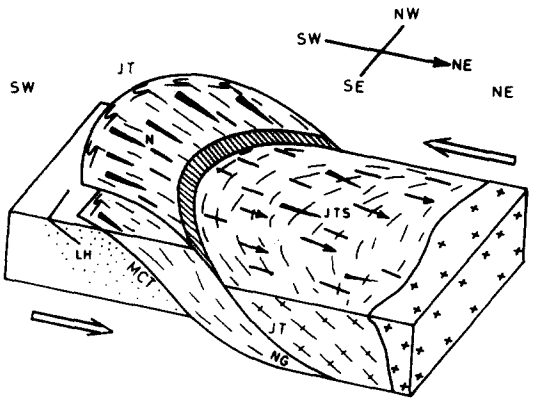

Fig. 17. Isometric diagram of the Central Crystalline Zone with extensive migration of the Jutogh Thrust Sheet (JTS) over the Naitwar Group metamorphics (N) along the Jutogh Thrust (JT). The Main Central Thrust (MCT) is concealed beneath the JT. Persistent NE-plunging F_2 folds (arrows) and mineral (thick lines)/stretching (long triangles) lineation. LH—Lesser Himalayan sedimentary zone. Crosses indicate the Harkidun granite gneiss.

Values of $\bar{\varepsilon}_s$ and ν also delineate such zones of high strain.

Graphically, strain parameters, k, K, ν and $\bar{\varepsilon}_s$ are discontinuous with distance near the tectonic boundaries along the Tons–Supin–Rupin Valleys. The spatial strain variations on logarithmic and Hsü diagrams are characterized by an increase in K and $\bar{\varepsilon}_s$ values towards plane strain field of strain ellipsoids during the D_2 deformational phase in the Central Crystalline Zone. Strain ellipsoids parallel the stretching lineation along the maximum extension direction and are genetically related to the propagation of the Central Crystalline units during the development of the shear zone. A strain cross-section through the Central Crystalline Zone reveal that the strain magnitude $\bar{\varepsilon}_s$ is mostly concentrated into narrow shear zones characterized by mylonite within a broad ductile shear zone at the deeper levels (Fig. 18a). As the ductile shearing moved upwards to higher structural levels, the shortening was accommodated by the development of thrust sheets from compound ductile zones with the thrust surfaces coinciding with zone of maximum shear strain and mylonite development (Fig. 18b).

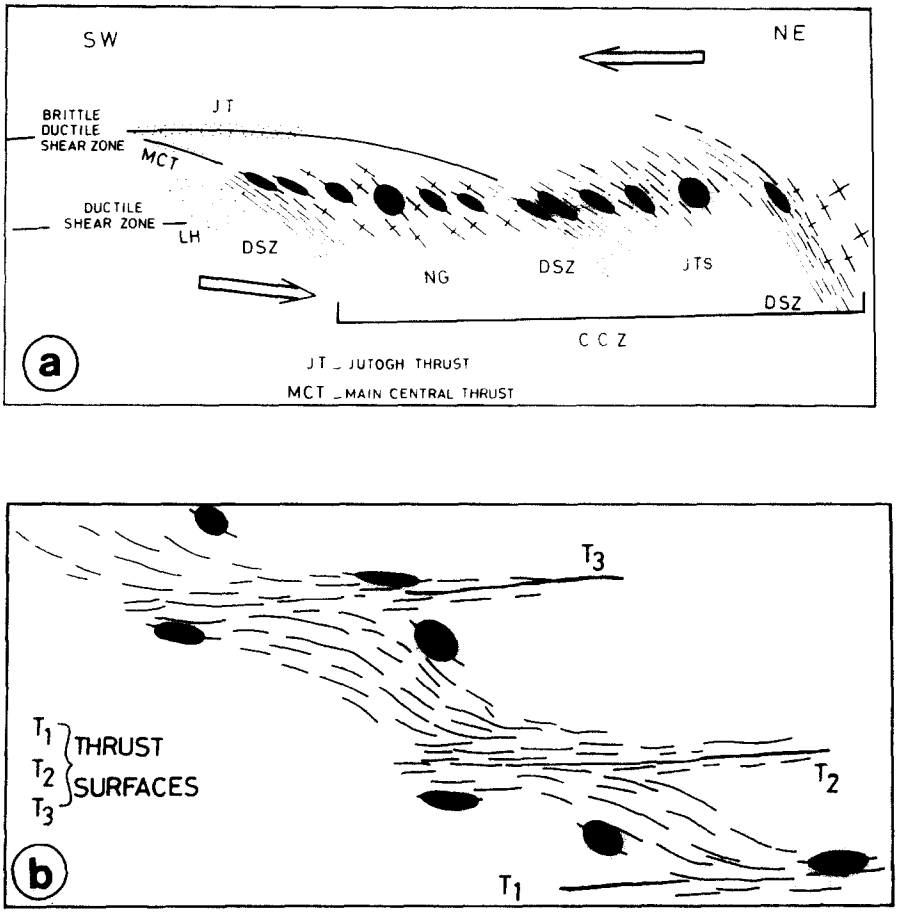

Fig. 18. (a) Strain cross-section and model of intracontinental crustal shortening of the Central Crystalline Zone. CCZ—Central Crystalline Zone as ductile shear zone. JTS—Jutogh Thrust Sheet, NG—Naitwar Crystalline Unit (Naitwar Group), DSZ—Ductile shear zone, LH—Lesser Himalayan sedimentary belt. R_s ratio of strain ellipses on XZ section exaggerated. (b) Ductile shear zone model of the thrust tectonics in the Central Crystalline Zone, NW Himalaya. Foliation trajectories in XZ section of compound ductile shear zone reveals maximum shear strain and development of mylonites in deeper levels and confinement of thrust surfaces (T_1, T_2, T_3) to the zones of maximum shear strain at shallower levels. R_s ratio of strain ellipses exaggerated.

The translation of the Central Crystalline Zone over the Garhwal Group is a continued crustal shortening phase during the late D_2 and D_3 deformational phases along the MCT and Jutogh Thrust which evolved from such zones of maximum strain. At higher levels, ductile shear zones are transformed into brittle–ductile and compressional zones (Ramsay 1980) which resulted in the development of NW–SE-plunging F_{3a} folds showing SW-vergence and almost orthogonal to the stretching fabric during the southward migration of thrust sheets. The youngest deformational phase is indicated by differential cooling and uplift of the metamorphic pile, as determined by the fission-track method, and in the development of lineaments, fractures and seismic activity, as a result of continuous northerly movement of the Indian Plate.

Acknowledgements—The authors are grateful to the Head of Department of Earth Sciences for kindly allowing the necessary facilities for these investigations, and to Prof. V. K. S. Dave for constant encouragement. The investigations form the major part of a Ph.D. thesis of one of the authors (Arvind Anand) and have been generously funded by the University Grants Commission, New Delhi. The work would not have been completed without the untiring assistance of R. C. Punj and Ram Dal in preparing the thin sections, Kamesh Gupta in drafting the figures, S. D Sharma in photography and Margaret Dias in typing the manuscript. Comments from Dr S. H. Treagus, Dr R. J. Lisle and Prof. S. K. Ghosh were very useful in improving and shortening the paper.

REFERENCES

Anand, A. 1986. Deformation and strain patterns of the Central Himalayan metamorphics from Northwestern Garhwal. Unpublished Ph.D. thesis, University of Roorkee, Roorkee, India.

Anand, A. & Jain, A. K. 1987. Earthquakes and deformational structures (seismites) in Holocene sediments from the Himalayan–Andaman Arc, India. *Tectonophysics* **133**, 105–120.

Berthé, D., Choukroune, P. & Jegouzo, P. 1979. Orthogneiss, mylonite and non-coaxial deformation of granites: the example of the South Armorican Shear Zone. *J. Struct. Geol.* **1**, 31–42.

Bhanot, V. B., Pandey, B. K., Singh, V. P. & Kansal, A. K. 1980. Rb–Sr ages for some granitic and gneissic rocks of Kumaun and Himachal Himalaya. In: *Stratigraphy and Correlations of Lesser Himalayan Formations* (edited by Valdiya, K. S. & Bhatia, S. B.). Hindustan Publication Corp., New Delhi, India, 139–142.

Bhargava, O. N. 1980. Outline of the stratigraphy of Eastern Himachal Pradesh, with special reference to the Jutogh Group. In: *Stratigraphy and Correlations of Lesser Himalayan Formations* (edited by Valdiya, K. S. & Bhatia, S. B.). Hindustan Publishing Corp., New Delhi, India, 117–125.

Bouchez, J. L. & Pecher, A. 1981. The Himalayan Main Central Thrust pile and its quartz rich tectonites in Central Nepal. *Tectonophysics* **78**, 23–50.

Boullier, A. M. 1986. Sense of shear and displacement estimates in the Abeibara–Rarhous late Pan-African shear zone, Adrar des Iforas, Mali. *J. Struct. Geol.* **8**, 47–58.

Brookfield, M. E. & Reynolds, P. H. 1981. Late Cretaceous emplacement of the Indus Suture zone ophiolitic melanges and an Eocene–oligocene magmatic arc on the northern edge of the Indian Plate. *Earth Planet. Sci. Lett.* **55**, 157–162.

Brun, J. P. & Pons, J. 1981. Strain patterns of pluton emplacement in a crust undergoing non-coaxial deformation, Sierra Morena, Southern Spain. *J. Struct. Geol.* **3**, 219–229.

Brunel, M. 1986. Ductile thrusting in the Himalaya: shear sense criteria and stretching lineation. *Tectonics* **5**, 247–265.

Burg, J. P., Guirand, M., Chen, G. M. & Li, G. C. 1984. Himalayan metamorphism and deformations in the Northern Himalayan Belt (Southern Tibet, China). *Earth Planet, Sci. Lett.* **69**, 391–400.

Carmignani, L., Giglia, G. & Kligfield, R. 1978. Structural evolution of the Apuane Alps: an example of continental margin deformation in the Northern Apennines, Italy. *J. Geol.* **86**, 487–504.

Choukroune, P. & Gapais, D. 1983. Strain pattern in the Aar Granite (Central Alps): orthogneiss developed by inhomogeneous flattening. *J. Struct. Geol.* **5**, 411–418.

Coward, M. P., Jan, M. O., Rex, D., Tarney, J., Thirlwall, M. & Windley, B. F. 1982. Geotectonic framework of the Himalaya of N. Pakistan. *J. geol. Soc. Lond.* **139**, 299–308.

Coward, M. P., Windley, B. F., Broughton, R., Luff, I., Petterson, M. G., Pudsey, C., Rex, D. & Khan, M. A. 1986. Collision tectonics in the N. W. Himalayas. In: *Collision Tectonics* (edited by Coward, M. P. & Ries, A.). *Spec. Publs geol. Soc. Lond.* **19**, 203–219.

Davidson, D. M. 1983. Strain analysis of deformed granitic rocks (Helikian) Muskoka District, Ontario. *J. Struct. Geol.* **5**, 181–185.

Dunnet, D. 1969. A technique of finite strain analysis using elliptical particles. *Tectonophysics* **7**, 117–136.

Elliott, D. 1970. Determination of finite strain and initial shape from deformed elliptical objects. *Bull. geol. Soc. Am.* **81**, 2221–2236.

Escher, A. & Watterson, J. 1974. Stretching fabrics, folds and crustal shortening. *Tectonophysics* **22**, 223–231.

Flinn, D. 1956. On the deformation of the Funzie Conglomerate, Fetlar, Shetland. *J. Geol.* **64**, 480–505.

Flinn, D. 1962. On folding during three dimensional progressive deformation. *Q. Jl geol. Soc. Lond.* **118**, 385–428.

Fry, N. 1979. Random point distribution and strain measurement in rocks. *Tectonophysics* **60**, 89–105.

Gansser, A. 1964. *Geology of the Himalayas*. Interscience Publishers, London.

Heim, A. & Gansser, A. 1939. Central Himalayas: geological observations of the Swiss Expedition 1936. *Mem. Soc. Helv. Sci. Nat.* **73**, 1–245.

Honegger, K., Dietrich, U., Frank, W., Gansser, A., Thoni, M. & Trommsdorf, V. 1982. Magmatism and metamorphism in the Lakakh Himalayas (the Indus–Tsangpo suture zone). *Earth Planet. Sci. Lett.* **60**, 253–292.

Hossack, J. R. 1968. Pebble deformation and thrusting in the Bygdin area (S. Norway). *Tectonophysics* **5**, 315–339.

Hsü, T. C. 1966. The characteristics of coaxial and non-coaxial strain paths. *J. Strain Anal.* **1**, 216–222.

Kligfield, R. 1979. The Northern Apennines as a collisional orogen. *Am. J. Sci.* **279**, 676–691.

Kligfield, R., Carmignani, L. & Owens, W. H. 1981. Strain analysis of a Northern Apennine shear zone using deformed marble breccias. *J. Struct. Geol.* **3**, 421–436.

Le Fort, P. 1981. Manaslu leucogranite: a collision signature of the Himalaya. A model for its genesis and emplacement. *J. geophys. Res.* **86**, 10,545–10,568.

Lisle, R. J. 1977. Estimation of tectonic strain ratio from the mean shape of deformed elliptical markers. *Geologie Mijnb.* **56**, 140–144.

Lisle, R. J. 1985. *Geological Strain Analysis: A Manual for the R_f/ϕ Method*. Pergamon Press, Oxford.

Mattauer, M. 1986. Intracontinental subduction, crust-mantle décollement and crustal-stacking wedge in the Himalaya and other collision belts. In: *Collision Tectonics* (edited by Coward, M. P. & Ries, A.). *Spec. Publs geol. Soc. London.* **19**, 37–50.

Nadai, A. 1963. *Theory of Flow and Fracture of Solids*. McGraw-Hill, New York.

Odling, N. E. 1984. Strain Analysis and strain path modelling in the Loch Tollier gneisses, Gairloch, NW Scotland. *J. Struct. Geol.* **6**, 543–562.

Pecher, A. 1977. Geology of the Nepal Himalaya: deformation and petrography in the Main Central Thrust zone. Colloq.Int. C.N.R.S., 268. *Ecologie et geologie de l'Himalaya*, 301–318.

Pecher, A. & Le Fort, P. 1986. The metamorphism in the Central Himalaya, its relation with thrust tectonic. *Mem. Sci. de la Terra* **47**, 285-309.

Pilgrim, G. E. & West, W. D. 1928. The structure and correlation of the Simla rocks. *Mem. geol. Surv. Ind.* **53**, 1–140.

Platt, J. P. & Behrmann, J. H. 1986. Structures and fabrics in a crustal-scale shear zone, Betic Cordillera, SE Spain. *J. Struct. Geol.* **8**, 15–33.

Ramsay, J. G. 1967. *Folding and Fracturing of Rocks*. McGraw-Hill, New York.

Ramsay, J. G. 1980. Shear zone geometry: a review. *J. Struct. Geol.* **2**, 83–89.

Ramsay, J. G. & Allison, I. 1979. Structural analysis of shear zones in an Alpinised Hercynian granite. *Schweiz. miner. petrogr. Mitt.* **69**, 251–279.

Ramsay, J. G. & Huber, M. I. 1983. *The Techniques of Modern Structural Geology*. Volume I: *Strain Analysis*. Academic Press, London.

Rhodes, S. & Gayer, R. A. 1977. Non-cylindrical folds, linear structures in the X direction and mylonite developed during translation of the Caledonian Kalak Nappe Complex of Finmark. *Geol. Mag.* **114**, 329–341.

Sanderson, D. J. 1973. The development of fold axes oblique to the regional trend. *Tectonophysics* **16**, 55–70.

Searle, M. P. 1986. Structural evolution and sequence of thrusting in the High Himalayan, Tibetan–Tethys and Indus suture zones in Zanskar and Ladakh, Western Himalaya. *J. Struct. Geol.* **8**, 923–936.

Siddans, A. W. B., Henrey, B., Kligfield, R., Lowrie, H. A. & Percevault, M. N. 1984. Finite strain patterns and their significance in Permian rocks of the Alps Maritime (France). *J. Struct. Geol.* **6**, 339–368.

Singh, R. P., Singh, V. P., Bhanot, V. B. & Mehta, P. K. 1986. Rb–Sr ages of the gneissic rocks of Rihee-Gangi, Bhatwari, Hanumanchatti and Naitwar areas of the Central Crystalline Zone of Kumaun Himalaya (U.P.). *Ind. J. Earth Sci.* **13**, 197–208.

Takagi, H. 1986. Implications of mylonitic microstructures for the geotectonic evolution of the Median Tectonic Line, central Japan. *J. Struct. Geol.* **8**, 3–14.

Tewari, A. P., Gaur, R. K. & Ameta, S. S. 1978. A note on the geology of a part of Kinnaur district, Himachal Pradesh. *Him. Geol.* **8**, 574–582.

Thakur, V. C. 1987. Development of major structures across the northwestern Himalaya, India. In: *Tectonic and Structural Process on a Macro-, Meso- and Micro-scale* (edited by Zwart, M., Martens, I. Van der Molen, Passchier, C. W., Spier, C. & Vissers, R. L. M.). *Tectonophysics* **135**, 1–13.

Trivedi, J. R., Gopalan, K. & Valdiya, K. S. 1984. Rb-Sr ages of granitic rocks within the Lesser Himalayan nappes, Kumaun, India. *J. geol. Soc. India* **26**, 641–654.

Williams, G. D. 1978. Rotation of contemporary folds into the X direction during overthrust processes in Laksefjord, Finmark. *Tectonophysics* **48**, 29–40.